# Assessment of membrane fouling indices during removal of reactive dye from batik wastewater

Indok Nurul Hasyimah Mohd Amin and Muhamad Hafiz Muhammad Nizam

## ABSTRACT

'Batik' is known as one of the most popular textile industries in Malaysia, and it produces wastewater in its processing. The wastewater contains reactive dye and is released into drains as well as rivers. It could cause harm to the environment and interrupt the food chain due to the chemicals contained in it. The aim of the present study is to determine the flux performance and modified fouling index using ultrafiltration (MFI-UF) by using different membrane materials, feed concentrations and feed chemistry. The sample was obtained from Romi Batik located at Chendering Terengganu. Two UF membranes were used, with the membrane materials made from cellulose acetate and polyvinylidene fluoride (PVDF). The permeate flux and fouling indices were investigated at the solution pH values of 3 and 7 for different concentrations. It was clearly observed that the highest percentage dye rejection and MFI-UF obtained at pH 7 using a PVDF membrane was a value of 85.3792% and 72,088 s/L$^2$, respectively. Overall results revealed that an ultrafiltration process can be used to treat reactive dye from textiles before it is channelled into the sea or rivers, and has great potential to be commercialized as a new alternative in dye wastewater treatment.

**Key words** | batik, index fouling, reactive dye, textile, ultrafiltration

**Indok Nurul Hasyimah Mohd Amin**
(corresponding author)
**Muhamad Hafiz Muhammad Nizam**
Section of Chemical Engineering Technology,
Universiti Kuala Lumpur Malaysian Institute of Chemical & Bioengineering Technology,
Lot 1988 Kaw. Perindustrian Bdr. Vendor, Taboh Naning,
Alor Gajah 78000,
Melaka,
Malaysia
E-mail: *nurulhasyimah@unikl.edu.my*

## INTRODUCTION

Dye pollutants from textile dye industries are an important source of environmental contamination. There are about 10,000 dyes currently used in the textile industry (Poon *et al.* 1999). It is estimated that 1–15% of the dyes are lost during processing and are released into wastewater. The release of this colored wastewater poses a major problem for the industry as well as a threat to the environment (Sauer *et al.* 2002).

Dye pollutants are generally resistant to biological degradation (Kuo & Ho 2001; Sun *et al.* 2002). The discharge of dyes into the environment is a concern for both toxicological and aesthetic reasons, as dyes impede light penetration, damage the quality of the receiving streams and are toxic to the food chain for organisms (Padmesh *et al.* 2006). The world-wide and high level of production normally generates colored wastewater and gives environmental concerns. Textile companies, dye manufacturing industries, paper and pulp mills, tanneries, electroplating factories, distilleries, food companies and a host of other industries discharge colored wastewater (McKay *et al.* 1998).

The methods of color removal from industrial effluents, including biological treatment, coagulation, flotation, adsorption, oxidation and higher filtration among the treatment options, appear to have considerable potential for the removal of color from industrial effluents. It has previously been reported that active carbons are considered as a well-known adsorption treatment for the removal of micro-pollutants (Faur-Brasquet *et al.* 2003). However, commercially available activated carbon is still considered expensive (Sourja *et al.* 2005). The first noticeable effect in the receiving water is the color, which not only causes an aesthetic impact, but can also interrupt photosynthesis, thus affecting aquatic life. Other effects are related to dye degradation products, including aromatic amines, which

doi: 10.2166/wrd.2016.072

are known to be toxic and potentially carcinogenic. Therefore, these wastewaters must be adequately treated before disposal.

A membrane filtration process will be used in this study instead of a common or typical treatment for wastewater. The membrane filtration process that will be used is ultrafiltration, because the pore sizes are extremely tiny and it has advantages over other methods. Due to the fine pore size and lack of discrimination between influents of these membrane filtration systems, a very high quality effluent emerges, so it will block or filter the dye effectively.

Basically, an ultrafiltration membrane is used as it rejects and separates high molecular weight solutes as well as suspended solids, colloids and macromolecules. The ultrafiltration separation mechanism is commonly attributed to geometry such as the pore size of the membrane. Due to the pore size of the common ultrafiltration membrane, it is very suitable for use in removing dye from wastewater. The ultrafiltration membrane system conserves energy with minimal operation and labor costs, and it has the ability to retain high concentration, minimizing disposal costs for a wide range of industries.

Thus, the main objective of this study is to determine the permeate flux and modified fouling index-ultrafiltration (MFI-UF) by using different membrane materials, different feed solutions (real and synthetic solutions) and a variety of solution chemistry. The existing modified fouling index ($MFI_{0.45}$) based on cake filtration uses a 0.45 μm microfilter to measure the particulate fouling potential of feed water. However, it is not sensitive to small colloidal particles. Incorporating these particles, the MFI using ultrafiltration (UF) membranes was proposed (Boerlage 2001). In this study, a suitable reference membrane for the MFI-UF test was investigated using cellulose acetate (CA) and polyvinylidene fluoride (PVDF). Furthermore, the percentage of dye rejection using the ultrafiltration process was also determined.

## MATERIALS AND METHODS

### Chemicals, membranes and experimental rig

The experiments were carried out with effluent obtained from Romi Batik (Chendering, Terengganu). Table 1 summarizes the characteristics of the feed solutions, while Figure 1 illustrates the physical appearance of two different concentrations of the batik effluent. The membranes were made of CA and PVDF. The properties of the membranes are shown in Table 2. New membranes were soaked in pure water overnight prior to each run in order to remove the preservative liquids before the membranes could be used. Experiments were performed using Millipore UHP 62 stirred cell, as shown in Figure 2.

**Table 1** | Characteristics of the feed solution

| Characteristic | |
|---|---|
| pH | 11.89 |
| Concentrations | 77 and 22 ppm |
| Physical characteristics | Blue solution<br>Concentrated color<br>Odorless |

### Fouling indices experiments

There were two different dye concentrations of batik effluent used in this study, taken from the first and third washing

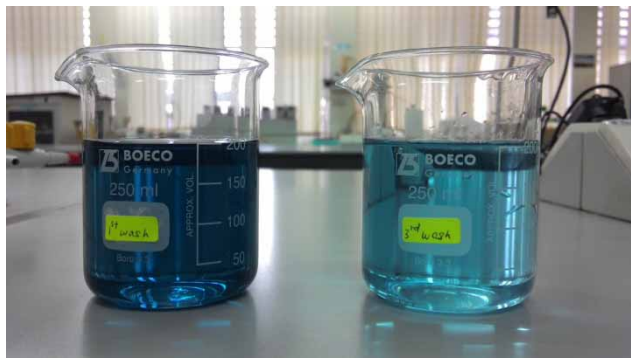


**Figure 1** | Batik wastewater for first and third wash.

**Table 2** | The properties of membranes

| Membrane | PVDF | CA |
|---|---|---|
| Manufacturer | Sterlitech | Sterlitech |
| Material | PVDF | CA |
| Surface property | Hydrophobic | Hydrophilic |
| Pore size | 0.20 μm | 0.22 μm |
| Thickness | ~125 μm | ~110 μm |

**Figure 2** | Ultrafiltration stirred cell unit.

process of batik. The first wash had high concentrations of dye (about 77 ppm), while the third wash had lower concentrations (about 22 ppm). This will give a range of the highest and lowest concentration of batik wastewater. The pH of the feed solution was altered to pH 3 and 7 with a few drops of 0.1 M HCl or 0.1 M NaOH by using a pH meter (Mettler Toledo). Compaction was performed to obtain a steady flux by passing 300 mL of ultra-pure water through the membrane at a pressure of 2.0 bar for 30 minutes prior to the experiment. Then, the solutions were added to the cell. Homogeneity was achieved by stirring the solution at 350 rpm in order to avoid the effect of concentration polarization. After the experiment was completed, the mixture was removed and the membrane surface was rinsed with pure water twice for 30 s. The flux of ultra-pure water through the membranes before and after the experiments was determined at transmembrane pressure (TMP = 1 bar). Permeate flux will be determined based on the volume collected, and can be calculated as Equation (1) (Majewska-Nowak 2009):

$$\textit{Permeate flux}\,(J) = \frac{V}{(A \times t)} \tag{1}$$

where $V$ is the volume of permeate at particular time ($L$), $A$ is the filtration area of the membrane ($m^2$) and $t$ is the duration of the filtration (h). Meanwhile, the dye rejection was calculated as a percentage according to the following equation:

$$\textit{Dye rejection}\ (\%) = \left(1 - \frac{C_p}{C_f}\right) \times 100\% \tag{2}$$

where $C_p$ is the permeate dye concentration and $C_f$ is the feed dye concentration (Alventosa-de Lara *et al.* 2012).

### Characterizations of the membranes after filtration

The changes on the surface morphology after experiments were visualized using scanning electron microscopy (SEM).

## RESULTS AND DISCUSSION

### Effect of feed concentration on membrane fouling performance

Basically there are two different feed concentrations that were run for the whole project: 77 and 22 ppm. Figures 3 and 4 show the ultrafiltration performance and particle size distributions, respectively.

Based on the results, the fouling that occurs for both of the membranes is at a concentration of 77 ppm, which can be determined by the permeate flux for each run. The permeate fluxes for 77 ppm clearly show a lower flux than 22 ppm. This was expected, because permeate flux decline was greater at higher concentrations, since as feed concentration increases, membrane fouling is more severe. An increase in dye adsorption on the membrane surface and concentration

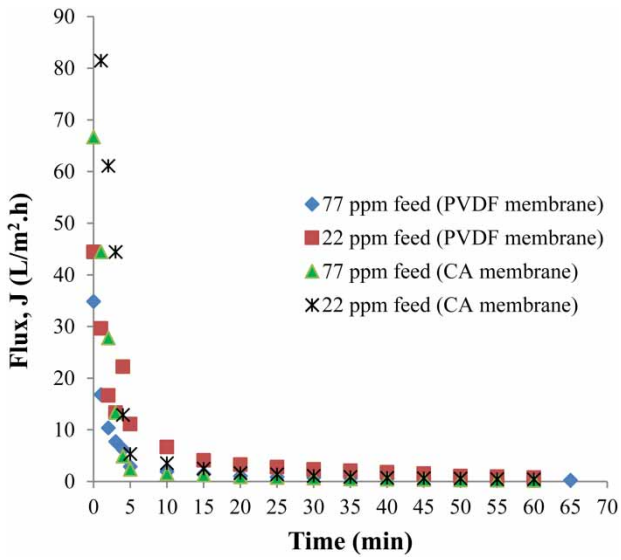


**Figure 3** | Flux performances at different feed concentrations.

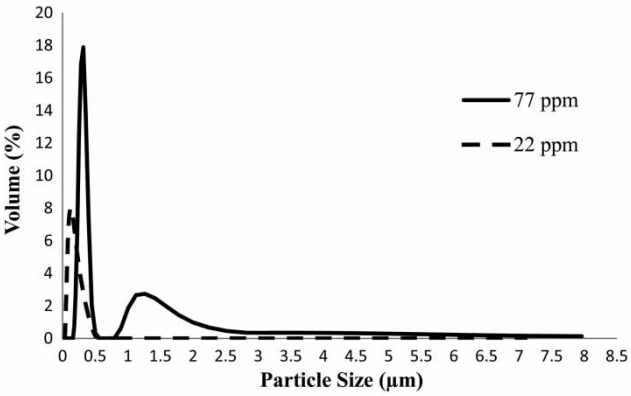


**Figure 4** | Particle size distributions of original solutions.

polarization might be the responsible factors for this observation (Chakraborty *et al.* 2003). The effect of feed concentration was more noticeable at 77 ppm for the PVDF membrane, where the *J* values were lower than others.

Furthermore, the particle size distribution of a particular concentration also plays an important role in fouling performance, as the membrane has a fixed pore size. The average particle size for 77 ppm was 0.292 μm, while for 22 ppm it was 0.138 μm. This explains why permeate flux declined drastically even at the beginning of the filtration. The particle size of 77 ppm exceeds the pore size of both membranes and causes clogging inside the pore faster than 22 ppm. The phenomenon of pore clogging can be clearly seen in Figures 5–7. All of the figures show the membranes in a clean and fouled condition.

Figure 5 exhibits the SEM images of a PVDF membrane. The image exhibits a porous surface structure with a large number of holes; they can also be labeled as not dense. Instead, the CA membrane pore patterns are denser than PVDF. Most of the dye only accumulated on the surface of the CA membrane, while for PVDF, it penetrated into the pores, which causes more dye rejection than CA (see Figures 6 and 7).

Overall, the results showed that permeate flux for the CA membrane was higher than permeate flux for the PVDF membrane due to its characteristics. The CA membrane was strongly hydrophilic and less prone to fouling, while the PVDF membrane was hydrophobic but more prone to fouling. Therefore, this explains why the CA membrane has high permeability compared to the PVDF membrane. Hence, it greatly affected the permeate flux.

## Effect of feed chemistry on membrane fouling performance

Figure 8 displays the relationship between flux and time for pH 7 and 3, whereas Figure 9 shows the particle size distributions at the original feed condition (pH 7) as well as in acidic conditions (pH 3). As shown in Figure 8, it is clear that the permeate flux for acidic conditions with the PVDF

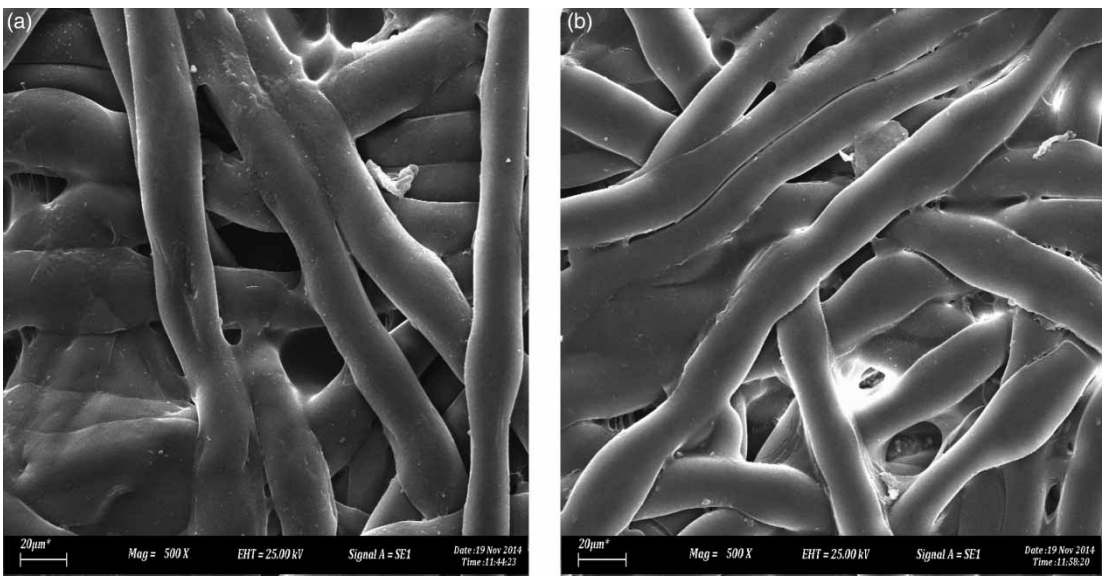


**Figure 5** | SEM images of clean (a) PVDF and (b) CA membranes.

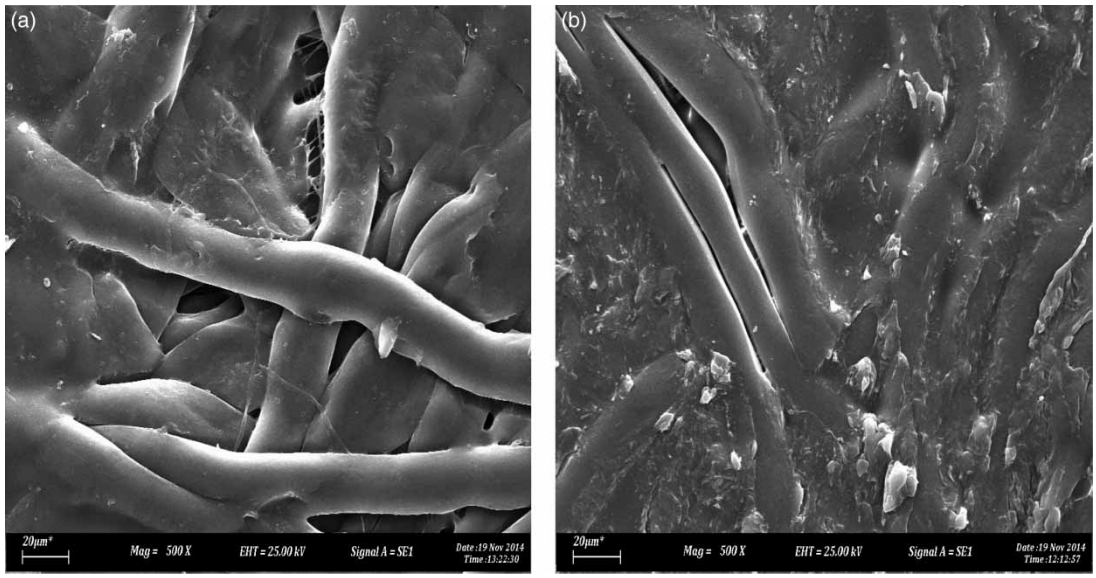


**Figure 6** | SEM images for fouled (a) PVDF and (b) CA membranes (at a concentration 77 ppm).

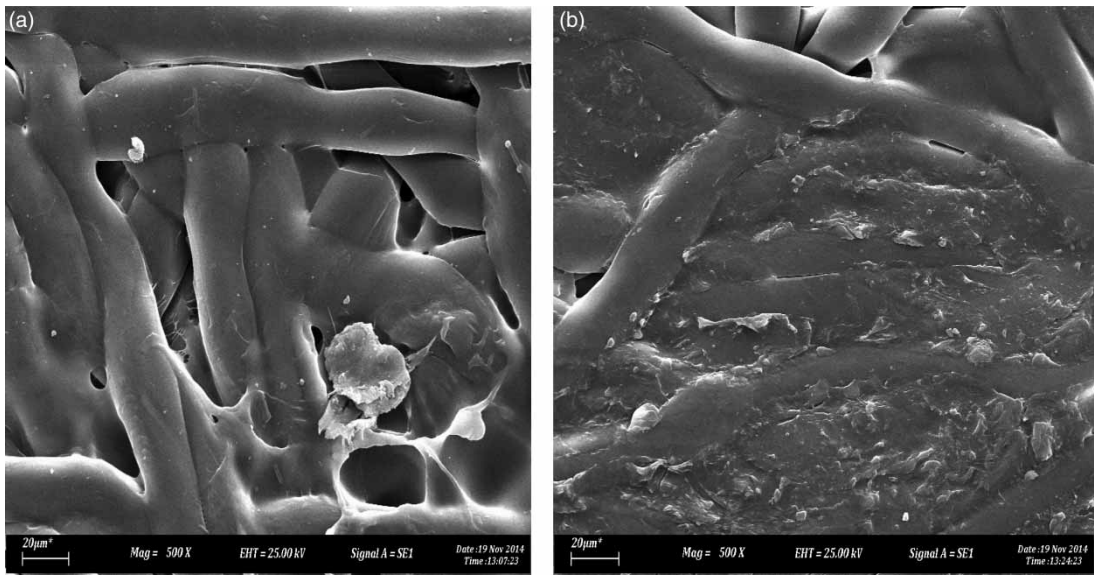


**Figure 7** | SEM images for fouled (a) PVDF and (b) CA membranes (at a concentration 22 ppm).

membrane was severely declined compared to the other conditions. This is due to the fact that it has a large particle size compared to pH 7. The particle size at pH 3 was 0.362 μm, while pH 7 was 0.196 μm, which can be clearly seen in Figure 9. Flux will surely decline due to membrane fouling. It is because the pore has been blocked, which reduces the permeate production rate and increases the complexity of the membrane filtration operation.

The membrane fouling that causes great flux decline can be seen in Figures 10 and 11. In the original feed solutions, the image clearly shows that a heavy clog occurred as the dye accumulated on the membrane surface after filling up the pores of the PVDF membrane. It is noticeable at pH 7 that the PVDF membrane did not display obvious deposition of dye particles on the pore structures. This is supported by the pore structure, as displayed in Figure 5.

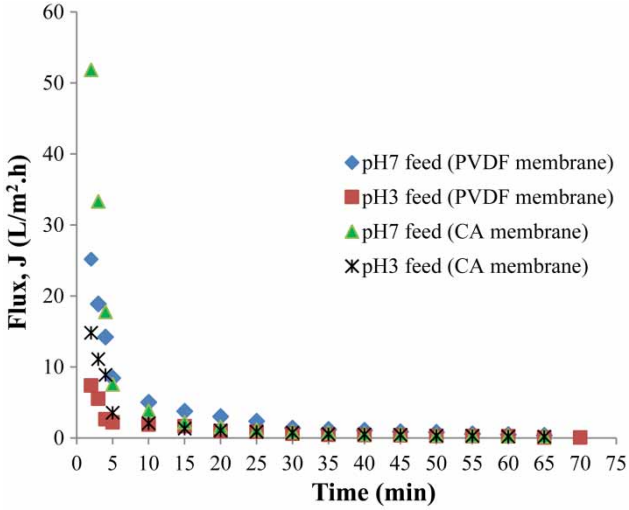


**Figure 8** | Flux performances at different pH.

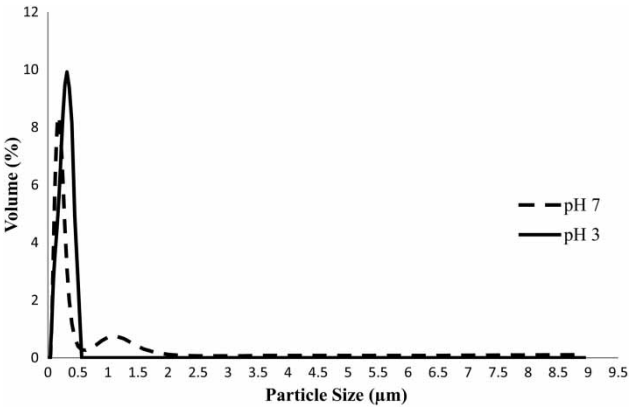


**Figure 9** | Particle size distributions at original and acidic feed chemistry.

Another reason for the flux decline was the formation of a cake layer on the surface of the membrane. The cake layer is formed on the membrane surface as the amount of retained particles increases. In addition, the cake layer creates an additional resistance to the permeate flow and the resistance of the cake layer increases with the growth of cake layer thickness. Hence, the permeate flux continues to decrease with time.

According to the flux performance reported in Figure 8, the higher flux is noticeable in acidic conditions for a CA membrane. This is because at lower pH the effect of concentration polarization and membrane fouling can be minimized (Ahmad *et al.* 2004).

## Determination of modified fouling index on membrane fouling

Figures 12 and 13 concisely summarize the results of the MFI for both CA and PVDF membranes. All the data were determined based on the gradient that was obtained from $1/Q$ versus volume of permeate, $V$.

Based on the results, it is shown that the value of MFI was higher for the PVDF membrane. It was noticeable that at pH 7, the indices were 72,088 s/L$^2$ for the PVDF membrane. This value was four times higher than the indices for the CA membrane, which was only 16,209 s/L$^2$. The MFI was very sensitive, and indicates the degree of membrane fouling whether it was heavily clogged or not.

The MFI values for all PVDF membranes were higher than the CA membranes. According to Figures 12 and 13, a huge gap between the MFI values of PVDF membranes and CA membranes is clearly shown. When the MFI value increased, the fouling of the membrane also increased. So, the fouling performance in PVDF membranes was higher and better than CA membranes.

## Percentage of dye rejection

The percentage of dye rejection is clearly presented in Figures 14 and 15 for both membranes and concentrations.

Figures 14 and 15 show the pattern of dye rejections at different feed concentrations and pH versus time. The figure concisely shows that the percentage of dye rejection increased with increasing time and feed concentration. This was due to faster formation of cake on the surface of the membrane. A gel layer that formed on the membrane surface could function as additional resistance to the dyes' permeation (Ahmad *et al.* 2006). Based on the 77 ppm for PVDF membranes, it is clearly shown that it has higher dye rejection compared to 22 ppm.

Higher dye concentration increased the dye accumulation on the membrane surface, and color removal became higher than those of the lower dye concentration. The highest dye rejection of 85.38% was achieved at pH 7 for the PVDF membrane. However, the dye rejection in acidic conditions can be measured only for the first 15 minutes of filtration. This is probably due to the severe decline showed by the membrane, which confirmed the formation

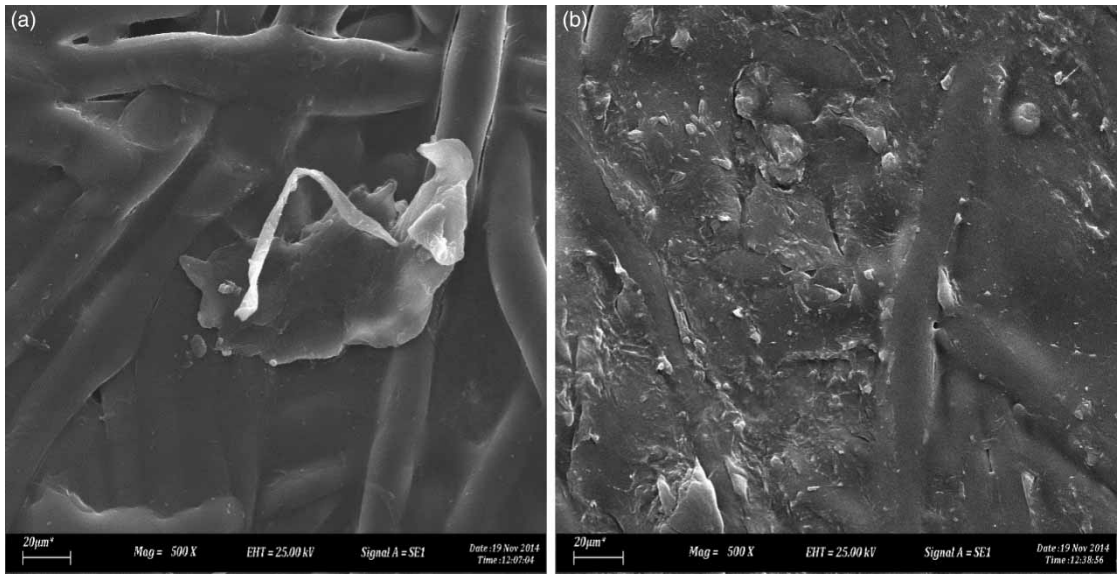


**Figure 10** | SEM images for fouled (a) PVDF and (b) CA membranes (at pH 7).

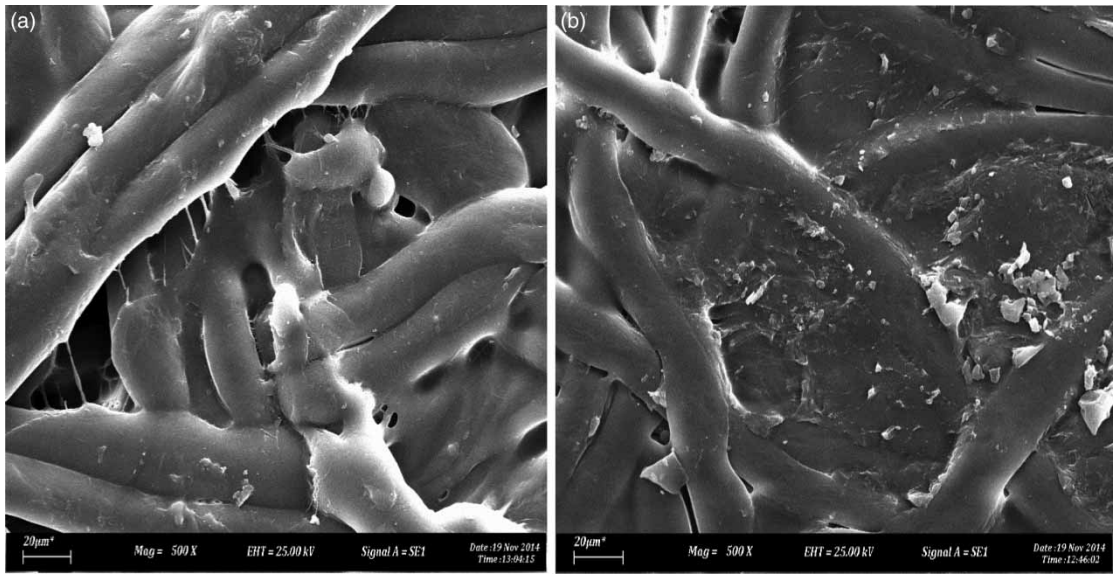


**Figure 11** | SEM images of pH 3 for fouled (a) PVDF and (b) CA membranes (at pH 3).

of large dye particles and its deposition on the pore structure by altering the chemistry to low pH levels.

Figures 16–23 clearly show the changes in physical appearance of the dye treatment after the filtration process.

It can be clearly seen that the color of the solution is highly concentrated in the first beaker and slowly turns to nearly colorless in the last beaker for all conditions and membrane materials. According to Cooper (1995), for the dyeing process, the safe pH of effluent to be released into water sources was in the range of 5–10. So, at pH 7 it meets the requirements for wastewater and is safe to be released. This claim is supported by the findings shown in Figure 15, in which the PVDF membrane could reject more than 80% of the dye from the initial concentrations

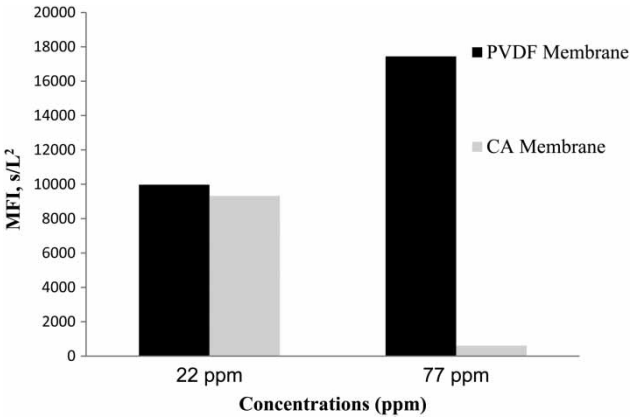


**Figure 12** | MFI values for different concentrations of solution.

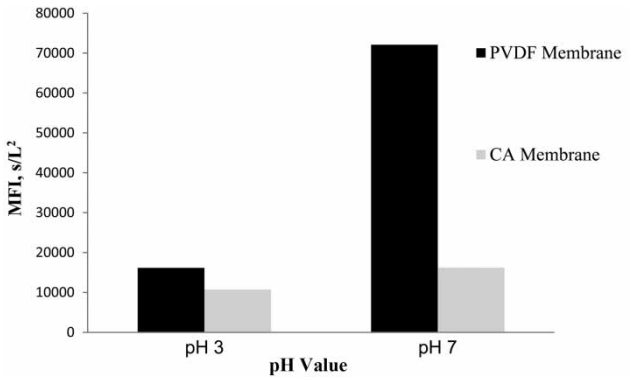


**Figure 13** | MFI values for different feed chemistry.

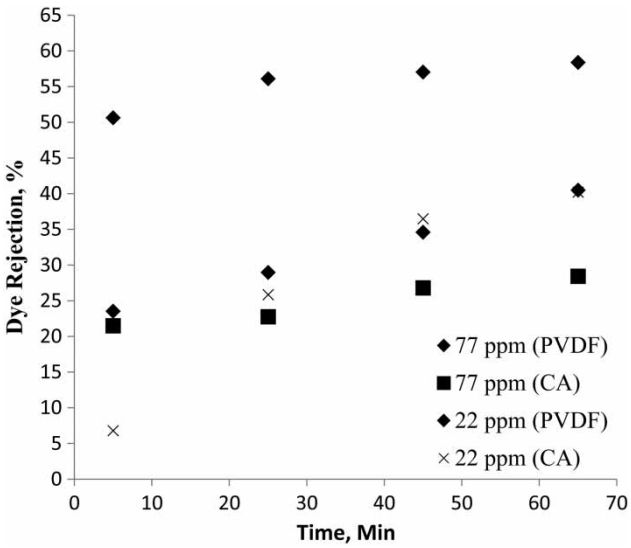


**Figure 14** | Dye rejections against time for different concentrations.

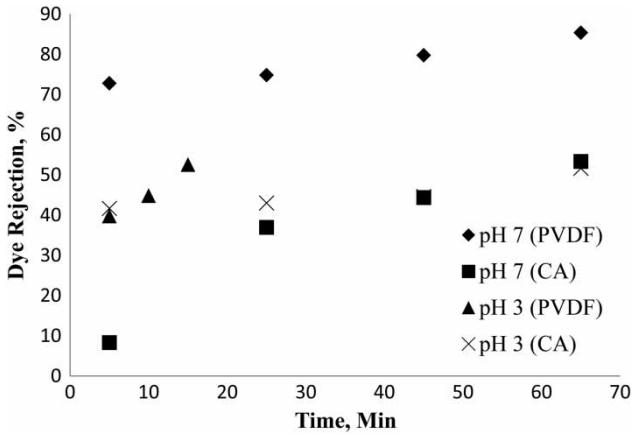


**Figure 15** | Dye rejections against time for different pH.

**Figure 16** | Wastewater color changes for pH 7 PVDF membrane after filtration.

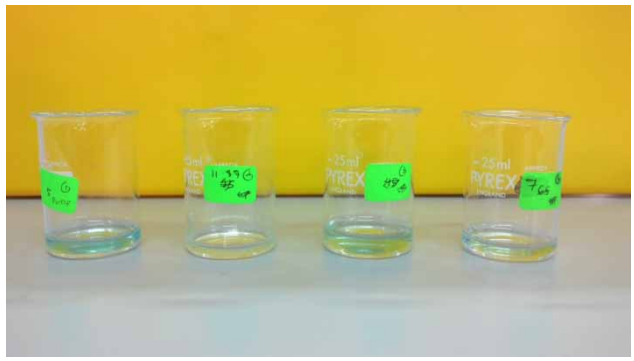

**Figure 17** | Wastewater color changes for 77 ppm PVDF membrane after filtration.

at pH 7 for 70 minutes of filtration. Moreover, the textile dyes have complex structures, synthetic origins and a recalcitrant nature, which requires their removal from industrial

**Figure 18** | Wastewater color changes for 22 ppm PVDF membrane after filtration.

**Figure 21** | Wastewater color changes for 22 ppm CA membrane after filtration.

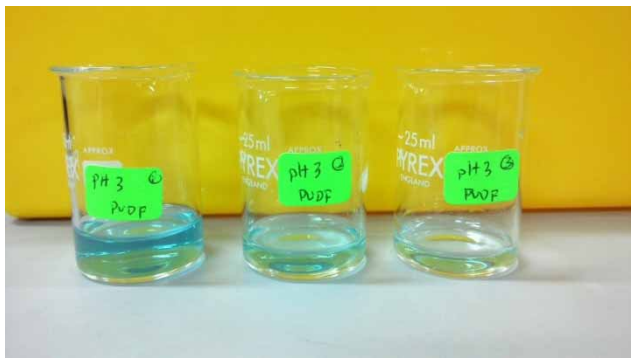

**Figure 19** | Wastewater color changes for pH 3 PVDF membrane after filtration.

**Figure 22** | Wastewater color changes for pH 7 CA membrane after filtration.

**Figure 20** | Wastewater color changes for 77 ppm CA membrane after filtration.

**Figure 23** | Wastewater color changes for pH 3 CA membrane after filtration.

effluents before being disposed into hydrological systems (Anjaneyulu *et al.* 2005).

Based on Figures 16–23, obviously the color concentration for the PVDF membrane was lighter than the CA membrane. Hence, the PVDF membrane was better than the CA membrane in filtering the dye at any feed concentration and pH value.

## CONCLUSIONS

The severe fouling during treatment of 'batik' wastewater has been investigated. It was due primarily to the deposition or adhesion of reactive dye on the membrane surface. Permeate flux and fouling indices have been used to

characterize the fouling performance. As a result, pH and feed concentrations play an important role in the ultrafiltration process. At a higher concentration and original pH, the cake formation on the membrane surface was predicted to be more dominant and led to extreme membrane fouling. The highest MFI (72,088 s/L$^2$) and dye rejection (85.38%) were achieved at pH 7 and 77 ppm feed concentration. Moreover, the surface chemistry of the membrane itself strongly affects the ultrafiltration process. PVDF was chosen as the best material because it can retain most of the dye on its surface. As the dye accumulation on the surface increased, the color removal also increased. The hydraulic efficiency of the membrane decreases and makes it more prone to fouling. As for the CA membrane, it contrasts with the PVDF as it is a strongly hydrophilic membrane that shows a high permeability and is less prone to fouling. Hence, it is not suitable for the process of dye filtration. The overall results show that the ultrafiltration membrane is feasible for significantly removing dye from wastewater.

## ACKNOWLEDGEMENTS

The authors gratefully acknowledge the financial support for this work by the UniKL MICET Short Term Research Grant (STRG) through grant no. str12059.

## REFERENCES

Ahmad, A. L., Bhatia, S. & Ibrahim, N. 2004 Removal of suspended solids and residual oil using membrane separation technology. In: *Regional Symposium on Membrane Science & Technology, April*. UTM, Johor Bahru, pp. 21–25.

Ahmad, A. L., Puasa, S. W. & Abiding, S. 2006 Crossflow ultrafiltration for removing direct-15 dye from wastewater of textile industry. *AJSTD* **23** (3), 207–216.

Alventosa-de Lara, E., Barredo-Damas, S., Alcaina-Miranda, M. I. & Iborra-Clar, M. I. 2012 Ultrafiltration technology with a ceramic membrane for reactive dye removal: optimization of membrane performance. *J. Hazard. Mater.* **209–210**, 492–500.

Anjaneyulu, Y., Sreedhara Chary, N. & Suman Raj, D. S. 2005 Decolourization of industrial effluents – available methods and emerging technologies – a review. *Rev. Environ. Sci. Biotechnol.* **4**, 245–273.

Boerlage, S. 2001 *Scaling and Particulate Fouling in Membrane Filtration Systems*. Taylor & Francis, Abingdon, Oxfordshire, pp. 118–126.

Chakraborty, S., Purkait, M. K., DasGupta, S., De, S. & Basu, J. K. 2003 Nanofiltration of textile plant effluent for color removal and reduction in COD. *Sep. Purif. Technol.* **31**, 141–151.

Cooper, P. 1995 *Color in Dyehouse Effluent*. Society of Dyers and Colourists, West Yorkshire, UK.

Faur-Brasquet, C., Cloirec, P. L. E. & Metivier-Pignon, H. 2003 Adsorption of dyes onto activated carbon cloth: approach of adsorption mechanisms and coupling of ACC with ultrafiltration to treat colored waste water. *Sep. Purif. Technol.* **31**, 3–11.

Kuo, W. S. & Ho, P. H. 2001 Solar photocatalytic decoloration of methylene blue in water. *Chemosphere* **45**, 77–83.

Majewska-Nowak, K. 2009 Ultrafiltration of dye solutions in the presence of cationic and anionic surfactants. *Environ. Protect. Eng.* **35** (4), 111–121.

McKay, G., Porter, J. F. & Prasad, G. R. 1998 The removal of dye colors from aqueous solution by adsorption on low-cost materials. *Water Air Soil Pollut.* **114**, 423–438.

Padmesh, T. V. N., Vijayaraghvan, K., Sekaran, G. & Velan, M. 2006 Biosorption of acid blue 15 using fresh water macroalga azola fuliculoids: batch and column studies. *Dyes Pigm.* **71**, 77–82.

Poon, C. S., Huang, Q. & Fung, P. C. 1999 Degradation kinetics of cuprophenyl yellow RL by UV/$H_2O_2$/ultrasonication (US) process in aqueous solution. *Chemosphere* **38** (5), 1005–1014.

Sauer, T., Neto, G. C., Jose, H. J. & Moreira, R. F. P. M. 2002 Kinetics of photocatalytic degradation of reactive dyes in a $TiO_2$ slurry reactor. *J. Photochem. Photoboil. A Chem.* **149**, 147–154.

Sourja, C., Sirshendu, D., Sunando, D. & Jayanta, K. B. 2005 Adsorption study for the removal of a basic dye: experimental and modelling. *Chemosphere* **58**, 1079–1086.

Sun, Z., Chen Ke, Y. Q., Yang, Y. & Yang, J. 2002 Photocatalytic degradation of cationic azo dye by $TiO_2$/bentonite nanocomposite. *J. Photochem. Photobiol. A Chem.* **149**, 169–174.

First received 19 June 2015; accepted in revised form 2 December 2015. Available online 13 January 2016